Research

Xanthatin nanocrystals exert anti-inflammatory properties against TNFα-primed 2D monolayers and in 3D spheroids of human HT29 colorectal cancer cells

Aleksandra Berenguer Roque[1] · Alain Zgheib[2] · Suslebys Salomon-Izquierdo[1] · Amanda Manso Peña[1] · Luis A. Osoria Alfonso[1] · Janet Piloto-Ferrer[1] · Borhane Annabi[2]

Abstract

Poor water-solubility of emerging new chemotherapeutic drugs lead to low absorption and tissue bioavailability. Improved drug delivery has therefore recently been achieved through the versatile physico-chemical properties of nanocrystals (NCs) in targeted cancer therapies. Here, nanocrystalization was used with xanthatin, a not highly water-soluble natural sesquiterpene lactone compound that possesses anti-tumour properties and which was recently investigated for potential use in the treatment of cancer and autoimmune diseases. Given that tumour-promoting inflammation is a hallmark of colorectal cancer (CRC), and that epidemiological studies associated inflammatory biomarkers to CRC poor prognosis and therapy resistance, the anti-inflammatory properties of xanthatin NCs were assessed in 2D monolayers and in 3D spheroids of a human HT29 CRC cell model. The 3D spheroids being a model recapitulating a cancer stem cells and chemoresistant phenotype. HT29 2D monolayer cell response was first tested against four pro-inflammatory inducers including phorbol-12-myristate-13-acetate, tumour necrosis factor alpha (TNFα), transforming growth factor beta, and Concanavalin A. Of these inducers, HT29 cell response to TNFα resulted in the most elevated expression of cyclooxygenase (COX)-2 which was prevented by commercial xanthatin along with the phosphorylation of the extracellular signal-regulated kinase 1/2 and of IkappaB (IκB). Alteration of 3D spheroids formation and of the inflammatory/immunity transcriptomic signature was also found better altered by xanthatin NCs in comparison to commercial xanthatin and the isolated molecule. Collectively, our data indicate that xanthatin nanocrystallization did not alter the potential in vitro anti-inflammatory and anticancer properties of xanthatin against a 3D CRC chemoresistance cellular model. These properties make NCs a significant advancement in the field of cancer theranostics to improve patient outcomes.

Keywords Chemoresistance · Colorectal cancer · Inflammation · Nanocrystals · Xanthatin

Abbreviations

AKT   Protein kinase B
ANGPT   Angiopoietin 2
BSA   Bovine serum albumin

✉ Borhane Annabi, annabi.borhane@uqam.ca | [1]Department of Experimental Oncology and Toxicology, Center for Pharmaceutical Research and Development, Havana, Cuba. [2]Chair in Cancer Prevention and Treatment, Département de Chimie, Université du Québec à Montréal, Succ. Centre-ville, Montreal, QC C.P. 8888, Canada.

Discover

cAMP	Cyclic adenosine monophosphate
ConA	Concanavalin A
CRC	Colorectal cancer
CSC	Cancer stem cell
COX-2	Cyclooxygenase 2
DMSO	Dimethylsulfoxide
DP	Dual plate
ECM	Extracellular matrix
EMT	Epithelial-to-mesenchymal transition
FasL	FAS ligand
Glut1	Glucose transporter 1
HIF1	Hypoxia-inducible factor 1
IL	Interleukins
NFκB	Nuclear Factor kappa B
PBS	Phosphate buffered saline
PGE2	Prostaglandin E2
PI3K	Phosphoinositide 3-kinase
PMA	Phorbol-12-myristate-13-acetate
RQV	Relative quantified value
RTCA	Real-time cell analyser
SCF	Stem cell factors
SEM	Standard error of the mean
TEAD	Transcriptional enhanced associate domain
TGFβ	Transforming growth factor beta
TME	Tumor microenvironment
TNFα	Tumour necrosis factor alpha
VEGF	Vascular endothelial growth factor
XRD	X-ray diffraction
YAP1	Yes-associated protein 1

1 Introduction

Tumors are not merely a simple aggregation of cells as they are composed of heterogeneous cancer cells and stromal cells that collectively create a complex tumor microenvironment (TME) [1]. In that context, inflammation plays a pivotal role in shaping the tumor's behavior, promoting pro-survival and pro-invasive factors, thereby facilitating tumour growth, metastasis, and resistance to therapy. The tumor-promoting inflammation represents a novel targeted therapeutic approach that aims to treat cancer from an immunological perspective [2, 3]. By harnessing this process, researchers are currently developing strategies to modulate inflammatory pathways, effectively activating the immune cellular responses against tumor development [4–6].

Phytochemicals are bioactive compounds produced by plants for their protection. They are classified according to their chemical structure and function in carbohydrates, phenols, lipids, alkaloids, terpenoids and other nitrogen-containing compounds [7]. Over the past few decades, phytochemicals have gained considerable interest as potential treatments for cancer due to their capacity to influence crucial biological pathways associated with tumor initiation, progression, and metastasis [8]. These compounds can selectively target cancer cells while minimizing harm to healthy tissues, positioning them as promising candidates for both preventive and therapeutic strategies [9]. These findings have resulted in numerous studies focusing on isolating these compounds from their natural sources or developing complete or semi-synthetic methods for obtaining them [10, 11].

Xanthatin is a natural sesquiterpene lactone isolated in the 1960s from *Xanthium strumarium* L., a native herb used in China that possesses a wide range of bioactivities, including anticancer, anti-inflammatory, anti-bacterial and anti-malarial activity [12]. Xanthatin was also reported to suppress proliferation and to induce apoptosis in a variety of tumor cell types, including A549 non-small cell lung cancer cells, human gastric carcinoma MKN-45 cells and human breast

cancer MDA-MB-231 cells [13, 14]. However, this type of phytochemical has shown limited pharmacokinetic properties, primarily due to their low bioavailability, which is a consequence of their poor solubility in water, resulting in suboptimal drug delivery [15–17]. Structural modifications and the chemical synthesis through complex routes of this compound have improved its physicochemical and pharmacological properties, thus enhancing its biological effects [18, 19].

Water insoluble or hydrophobic cancer drugs, represent a challenge in terms of achieving optimal bioavailability and thereby, adequate efficacy. It is estimated that around 75% of new drug candidates have poor water solubility, and many of these are anticancer drugs [20]. Nanocrystals (NCs) are a class of solid dosage forms that utilize the concept of nanoscience together with crystal nature of drugs to achieve advantages in terms of solubility, dissolution, and physicochemical properties. The reduction of the particle size to a nanometer range provides an enhanced surface area and gives enhanced dissolution rate, saturation solubility, increased cell membranes/surface adhesiveness, and oral bioavailability. Thus, NCs show the fast onset of action, minimum adverse effects, high drug load, multiple administration routes, minimized drug concentration, and an overall enhancement in the safety and efficiency of the drug molecule [21, 22].

Our prior research has substantiated the efficacy of the metabolite xanthatin as an anti-tumour agent [23–25]. As we previously reported, the molecule has been shown to play a role in triggering apoptotic mechanisms, inhibiting cell proliferation and effectively targeting the invasive phenotype in several cell models, including ovarian and colorectal [23–25]. In this study, we aimed to ascertain the differences in antitumour efficacy between xanthatin, isolated from the Cuban plant species *Xanthium strumarium* L., presented as crystals and NCs by targeting specific tumor promoting inflammation biomarkers in two-dimensional (2D) monolayers and three-dimensional (3D) spheroids of a human HT29 colorectal cancer (CRC) cell model. The nanocrystallization process significantly enhances the physicochemical properties of active pharmaceutical ingredients by effectively reducing their particle size. Considering the aforementioned points, an improvement in efficacy and a more pronounced biological effect of our target metabolite is expected.

2 Materials and methods

2.1 Reagents

Isolated xanthatin (MW = 246.30 g/mol; 98,4% purity; particle size 300 μm) and xanthatin nanocrystals (NCs) (particle size 669 nm) were obtained from the Department of Experimental Oncology and Toxicology at the Center for Pharmaceutical Research and Development (PCT/CU2024/050007, CIDEM; Havana, Cuba). Briefly, xanthatin NCs were obtained using the antisolvent precipitation technique. For this, xanthatin isolated from *Xanthium strumarium* was dissolved in ethanol and added surfactant. The resulting suspension was centrifuged, the precipitate was resuspended and finally lyophilized. The obtained NCs were characterized through residual moisture analysis, melting point determination, particle size measurement, X-ray diffraction (XRD), scanning electron microscopy, and Fourier transform infrared (FTIR) spectroscopy, confirming that all the evaluated physicochemical parameters were adequate. Commercial xanthatin was purchased from APExBIO (Houston, TX, USA). Dimethylsulfoxide (DMSO), Bovine serum albumin (BSA), transforming growth factor beta (TGFβ), Concanavalin A (ConA), tumor necrosis factor alpha (TNFα) and protease inhibitor cocktail were from Sigma-Aldrich (Oakville, ON, Canada). Trypan Blue reagent was from Bio-Rad (CAT: 14,550,013, The Junction Station Road, WAT, UK). Micro bicinchoninic acid protein assay reagents were from Pierce (Rockford, IL, USA). Electrophoresis reagents were from Bio Basic (Markham, ON, Canada). The Clarity™ Western ECL Substrate for horseradish peroxidase (HRP)-conjugated antibody detection reagents were from Bio-Rad (Hercules, CA, USA). The polyclonal antibodies against IκBα (4814S), phospho-IκBα Ser32/36 (9246S) and p44/42 MAPK (ERK1/2), and the monoclonal antibody against GAPDH (D4C6R), phospho-p44/42 MAPK (ERK1/2) were from Cell Signaling Technology (Danvers, MA, USA).

2.2 2D monolayer cell culture

Human HT29 colorectal adenocarcinoma cell line was purchased from the American Type Culture Collection (ATCC; Manassas, VA, USA). HT29 cells were cultured in McCoy's 5a 1X Modified Medium (Wisent, CAT: 317-010-CL, St-Jean-Baptiste, QC, Canada) supplemented with 10% fetal bovine serum (FBS; HyClone Laboratories, SH30541.03) and 100 U/ml penicillin, 100 μg/ ml streptomycin antibiotics (Wisent, CAT: 450-201-EL). Cells were maintained under standard cell culture conditions at 37 °C and 5% CO_2 in a humidified incubator and passaged when reached 70–90% confluency 2–3 times per week.

2.3 3D spheroid cellular model

HT29 3D spheroids were generated by the hanging drop technique on petri dishes [26]. Cells were first cultured in growth media until 70–80% confluency was reached, then detached with 0.05% trypsin/EDTA (Wisent, CAT: 325-042-CL). After trypsin inactivation, the resulting single cells were washed twice in pre-warmed complete media. Dissociated single cells were re-suspended in McCoy's 5a 1X complete Modified Medium as 10^6 cells/mL and 40 μL of the cell suspension was taken for a final concentration of 4×10^4 cells. About 40×40 μL cellular drops were dispensed on the inverted lids of 100 mm petri dishes and the lids were carefully set on the dishes, which had been pre-filled with 5 mL of sterilized water to assure high humidity. Spheroids were treated with either vehicle or 0.3, 1, 3 μM of commercial xanthatin, isolated xanthatin or xanthatin NCs and allowed to aggregate and self-organize for a period of 4 days. The spheroids were maintained at 37 °C, in a humid atmosphere with 5% CO_2. Following the 4 days incubation period, the morphology of the treated spheroids was analyzed, and the resulting micrographs were acquired and processed with NIS Element (Nikon, Japan) and ImageJ (U.S. National Institutes of Health, Bethesda, MD, USA) software packages. Reduction in spheroid size after xanthatin treatment was considered based on the difference in sizes between untreated control spheroids and xanthatin-treated spheroids.

2.4 Cytotoxicity assay

Trypan Blue dye exclusion assay was used to determinate the cytotoxic effect of xanthatin on HT29 cell viability. Cells were plated in a 24-wells plate for 24 h to allow cell adherence. After this period, control, commercial xanthatin, isolated xanthatin and xanthatin NCs were added to serum-free cell culture media at different concentrations (0.1, 0.3, 1 and 3 μM) for 24 h. Upon xanthatin treatment, cells were detached with 0.05% trypsin/EDTA (Gibco, Germany) and after trypsin inactivation, the resulting cell suspension was obtained in a fixed volume of cells (1 ml). Ten μl of cell suspension was taken and mixed with an equivalent volume of trypan blue dye. The mixture was transferred to a hemocytometer to count the number of viable cells for each treatment per concentration. Total number of cells, live cells and percent of live cells were registered in each case. The assay was performed in triplicate for each test group. The viability was expressed as the percent of viable cells against control (untreated) cells by using formula: % viability = (live cell count/total cell count) *100.

2.5 Total RNA isolation, cDNA synthesis, and real-time quantitative PCR

Total RNA was extracted from cell monolayers or spheroids using 1 mL of TriZol reagent (Life Technologies, Gaithersburg, MD, USA). Two μg of total RNA was reverse-transcribed for cDNA synthesis using a high-capacity cDNA reverse transcription kit (Applied Biosystems, Foster City, CA) or, in the case of the gene array, the R^2 First Strand kit (QIAGEN, Valencia, CA, USA). Prior to PCR, the cDNA was kept at − 80 °C. Real-time quantitative PCR was used to measure gene expression using iQ SYBR Green Supermix (Bio-Rad, Hercules, CA, USA). The Icycler iQ5 (Bio-Rad) was used for DNA amplification, and product identification was assessed by detecting the binding of the fluorescent dye SYBR Green I to double-stranded DNA. The following primer sets were from QIAGEN: GAPDH (Hs_GAPDH_1_SG, QT00079247), Peptidylprolyl Isomerase A (PPIA) (Hs_PPIA_4_SG, QT01866137), β-Actin (Hs_Actb_2_SG, QT01680476), (COX)-2 (Hs_PTGS2_1_SG, QT00040586), GLUT1 (Hs_SLC2A1_1, QT00068957), VEGF (Hs_VEGFA_1, QT01010184), HIF1 (Hs_H1F1_1_SG, QT00083664), YAP1 (Hs_YAP1_1_SG, QT000080822) and TEAD (Hs_TEAD1_1_SG, QT00009421). The relative quantities of target gene mRNA were normalized against two internal housekeeping genes *PPIA* and *GAPDH*. The RNA was measured by following a ΔC_T method employing an amplification plot (fluorescence signal vs. cycle number). The difference (ΔC_T) between the mean values in the triplicate samples of target gene and the housekeeping genes was calculated with the CFX manager Software version 2.1 (Bio-Rad) and the relative quantified value (RQV) was expressed as $2^{-\Delta CT}$.

2.6 Human inflammatory cytokines and receptors, and human transcription factors qPCR arrays

The RT^2 Profiler™ PCR arrays for Human Inflammatory Cytokines and Receptors (PAHS-181Z) and for Human Transcription Factors (PAHS-075ZD) were used according to the manufacturer's protocol (QIAGEN). The detailed list of the key genes assessed can be found on the manufacturer's website (https://geneglobe.qiagen.com/us/product-groups/rt2-profiler-pcr-arrays). Using real-time quantitative PCR, we analyzed the expression of a focused panel of genes related to the inflammatory response and a cluster of transcription factors associated with epithelial-to-mesenchymal transition (EMT),

inflammation and invasive phenotype. Relative gene expression was calculated using the $2^{-\Delta\Delta CT}$ method ("delta-delta" method). This method normalizes the ΔC_T value of each sample using five housekeeping genes (*B2M*, *HPRT1*, *RPL13A*, and *GAPDH*). The normalized FC values were then presented as average FC = 2 (average$^{\Delta\Delta C}$T). The resulting raw data were then analyzed using the PCR Array Data Analysis Template (http://www.sabiosciences.com/pcrarraydataanalysis.php). This integrated web-based software package automatically performs $\Delta\Delta C_T$-based FC calculations from the uploaded raw thresholded cycle data.

2.7 Western blots

HT29 cells were cultured in complete McCoy's 5a 1X Modified Medium (Wisent, CAT: 317-010-CL) for 24 h, followed by treatment with 1 μM PMA, 30 ng/mL TNFα, 1 μM TGFβ or 30 μg/mL ConA in serum free media in the presence or absence of 3 μM commercial xanthatin to evaluate the extent of COX-2 expression. In a separate experiment and given that HT29 cells were significantly more responsive to TNFα, cells were treated with TNFα (30 ng/mL) in serum free media in the presence or absence of 0.3 μM of commercial xanthatin, isolated xanthatin and xanthatin NCs for 30 min for phospho-ERK/ERK expression and for 5 min for phospho-IκB/IκB determination. Subsequently, serum-starved HT29 cells were treated with xanthatin NCs (1 and 3 μM) for 24 h. After this, cells were stimulated with TNFα (30 ng/mL) for the indicated times (2, 5, 10, 30, and 60 min). Cells were then collected for Western blot analysis. The total cellular protein content was extracted by RIPA buffer (1 mM sodium fluoride, 1 mM sodium orthovanadate, 1X protease inhibitor cocktail). Total protein concentration was quantified by the BCA method. Equal amounts of protein (20 μg) were separated by SDS-PAGE 10% polyacrylamide gel electrophoresis and then electro-transferred onto a low fluorescence polyvinylidene difluoride (PVDF) membrane (Merck Millipore, Carrigtwohill, CO, Ireland). The membranes were blocked with 5% non-fat dry milk in 100 mM Tris–HCl (pH 7.5), 150 mM NaCl, and 0.3% Tween-20 (TBST; Bioshop, TWN510-500) for 1 h at room temperature and then washed thrice with TBST for 15 min each time, finally the membranes were incubated overnight at 4 °C with agitation with the corresponding primary antibodies (1/1000 dilution) in TBST containing 3% BSA and 0.1% sodium azide (Sigma Aldrich). The next day, after three more washes with TBST, the membranes were incubated with the appropriate horseradish peroxidase-conjugated secondary antibodies for 1 h at room temperature. The antigen was detected using Clarity™ Western ECL Substrate (ECL). The images were acquired on a ChemiDoc™ XRS + Imaging System (Bio-Rad) using ImageLab software.

2.8 Real-time cell migration assay

Cell migration analysis of HT29 cells was performed using the Real-Time Cell Analyser (RTCA) Dual-Plate (DP) instrument and the xCELLigence System (Roche Diagnostics, QC, Canada). For the analysis 25,000 cells per well were seeded in a CIM-plate (Roche Diagnostics) and incubated at 37°C under a humidified atmosphere containing 5% CO_2 for 24 h. Prior to cell seeding, the bottom of each well in the upper chamber was coated with 0.15% gelatin in phosphate buffered saline (PBS) and incubated for 1 h at 37°C. The lower chamber was filled with serum free medium containing either the vehicle, TNFα only or commercial xanthatin, isolated xanthatin or xanthatin NCs at different concentrations (0.1, 0.3, 1 and 3 μM). The upper chamber of each well was filled with 25,000 cells, in serum-free media as well. After 30 min of initial adhesion, cell migration was monitored for up to 7 h. The impedance value was measured by the RTCA DP instrument and expressed as an arbitrary unit called the Cell index. Each experiment was performed in quadruplicate Wells. Data and error bars were expressed as mean ± standard error of the mean (SEM).

2.9 Statistical data analysis

Data and error bars were expressed as the mean ± SEM of two to three independent experiments. Hypothesis testing was conducted using a Mann–Whitney U-test (for comparison of two groups) with probability (P) values of less than 0.05 (*) considered significant and denoted in the respective figures. All statistical analysis were performed using the GraphPad Prism 7 software version 9.0.0 (GraphPad Software LLC, San Diego, California, USA).

3 Results

3.1 In vitro cytotoxic evaluation of commercial xanthatin, isolated xanthatin and xanthatin nanocrystals on human HT29 colorectal cancer cells

To screen for the in vitro cytotoxic properties of xanthatin, Trypan Blue exclusion assay was performed. HT29 CRC cells were cultured as stated in the Methods section and were subjected to treatment with increasing concentrations (0.1, 0.3, 1 and 3 µM) of commercial xanthatin, isolated xanthatin and xanthatin NCs for 24 h. The cytotoxic activity of the molecule was expressed as the percent of living cells compared to the control. As illustrated in Fig. 1A, the administration of commercial xanthatin did not result in a notable reduction of cell survival at the various concentrations tested, with only a slight impact on cell viability was observed at the highest concentration tested 3 µM. The minimum effective concentration for both isolated xanthatin and the NCs was 0.3 µM, at which point a non-statistically significant differential effect on HT29 cell viability could be quantified. However, the isolated xanthatin and xanthatin NCs displayed higher inhibitory effects, exhibiting significant greater potency to reduce cell viability to approximately 30% of control at a concentration of 3 µM.

3.2 Xanthatin significantly inhibits COX-2 protein expression in HT29 cells stimulated with pro-inflammatory inducers PMA, TNFα, TGFβ and ConA

The aim of this study was to first ascertain whether xanthatin treatment could mitigate the expression of the pro-inflammatory marker COX-2 in HT29 colorectal cancer cells triggered by different inflammatory cues. For this purpose, HT29 cells were stimulated with four pro-inflammatory inducers, namely 1 µM PMA, 30 ng/mL TNFα, 1 µM TGFβ or 30 µg/mL ConA, and treated in serum-free media in the presence or absence of 3 µM commercial xanthatin. Proteins from cell extracts were analyzed by Western blotting for COX-2 expression. Figure 2A illustrates a representative pattern of cellular response to the four inducers of inflammation employed.

　　HT29 cells exhibited an ~ 10 × increase in responsiveness to TNFα treatment in comparison to the other inducers, as reflected by a notable increase in COX-2 protein expression. PMA and TGF treatments resulted in a moderate ~ 4 × response, while ConA remained ineffective. It was therefore decided to continue with only TNFα as an inflammation inducer for subsequent experiments. Densitometric analysis from a representative immunoblot revealed that xanthatin treatment was effective in attenuating the induced overexpression of COX-2 at the protein level (Fig. 2B). In addition, RT-qPCR was performed to validate Western blotting results for the inhibition of COX-2 upon treatment with TNFα in the presence or absence of 3 µM commercial xanthatin, confirming that the administration of xanthatin

Fig. 1 In vitro cytotoxic evaluation of commercial xanthatin, isolated xanthatin and xanthatin nanocrystals on human HT29 colorectal cancer cells. HT29 cell monolayers were treated with the indicated concentrations of commercial xanthatin, isolated xanthatin or xanthatin nanocrystals in serum-free media for 24 h. **A** A Trypan Blue exclusion assay was performed in triplicate as described in the Methods section. A representative cytotoxicity profile is presented and expressed as the percent of viable cells against control vehicle-treated cells (*$p < 0.05$)
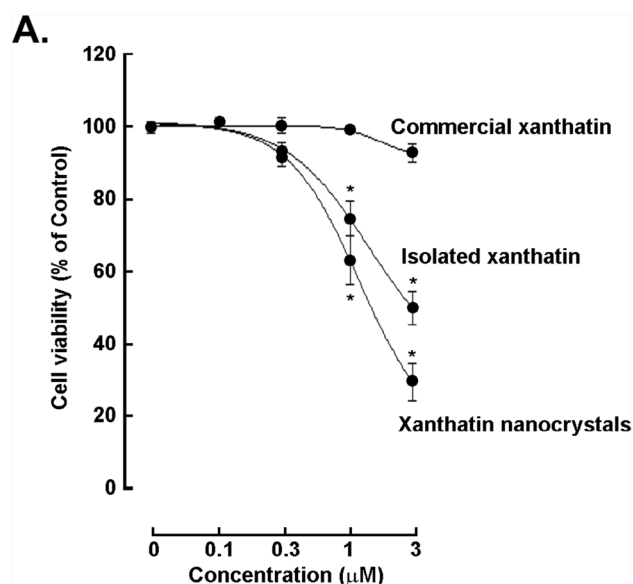
Fig. 2 Xanthatin significantly inhibits COX-2 protein expression in HT29 cells stimulated with proinflammatory inducers PMA, TNFα, TGFβ and ConA. HT29 colorectal cells were treated with 1 μM PMA, 30 ng/mL TNFα, 1 μM TGFβ or 30 μg/mL ConA in serum free media in the presence or absence of 3 μM commercial xanthatin. **A** Cell lysates were harvested, and immunoblotting analysis was performed as described in the Methods section. **B** A representative densitometry analysis was conducted to evaluate the extent of COX-2 expression triggered by PMA, TNFα, TGFβ, and ConA, and the impact of 3 μM xanthatin in attenuating this response. The relative expression of COX-2 was quantified and normalized to GAPDH. **C** Relative gene expression levels were then assessed by RT-qPCR for COX-2 expression. Data are expressed as gene expression fold increase over control in TNFα- or TNFα plus xanthatin-treated cells (*$p < 0.05$)
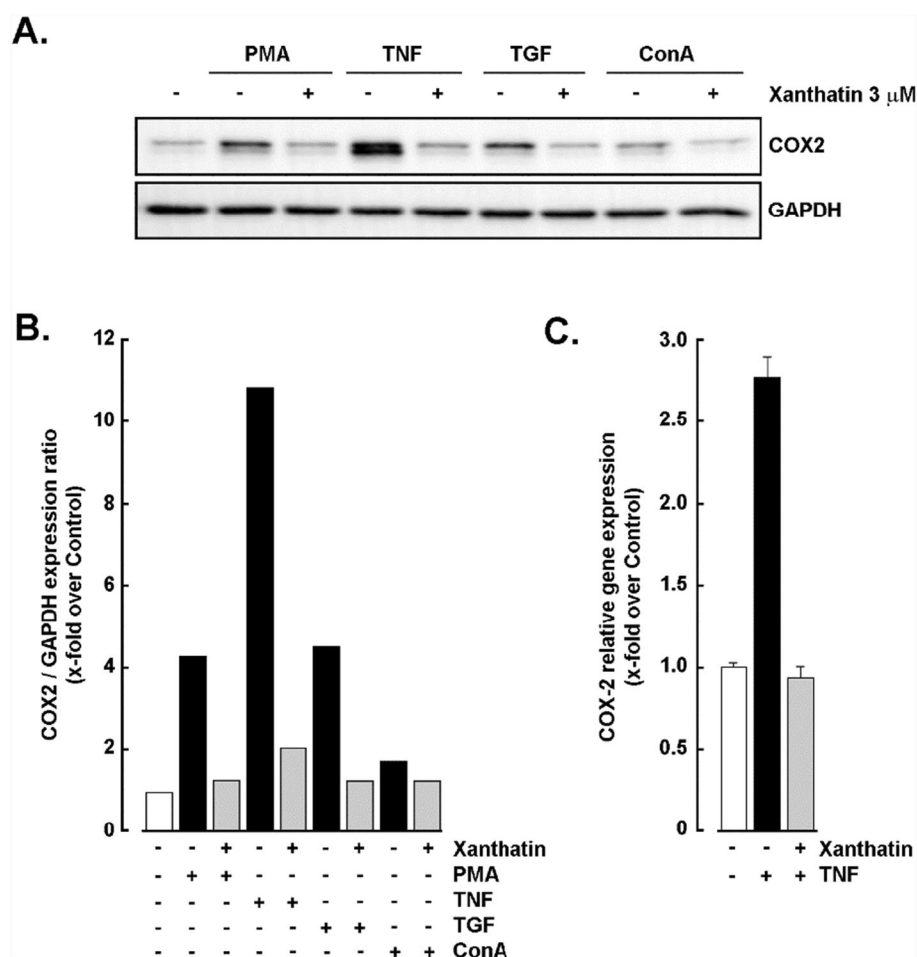

reduced or completely abrogated the over-expression of COX-2 transcript levels (Fig. 2C), restoring the protein expression levels to a state close to the baseline.

3.3 Effect of commercial, isolated and nanocrystallized xanthatin on the formation of 3D HT29-derived spheroids

The effects of commercial, isolated and nanocrystallised xanthatin on the formation of tumour spheroids derived from the human colorectal cancer line HT29 was evaluated by considering variations in size and morphology compared to the control group. For this purpose, the diameters of spheroids exposed to commercial xanthatin (Fig. 3A), isolated xanthatin (Fig. 3B), and xanthatin NCs (Fig. 3C) were measured after 4 days of incubation with the treatment. Three replicates per treatment per group were considered. Phase contrast microscopic observations showed morphological alterations in response to xanthatin treatment; while the spheroids of the control group were more condensed, larger and presented a regular and uniform spherical shape. The spheroids of the groups treated with commercial, isolated and xanthatin NCs showed considerable morphological variations such as reduction in size, loss of compactness and integrity according to the concentration tested (Fig. 3D). Whereas no effect on spheroids size was observed at 0.3 μM of either commercial or isolated xanthatin, xanthatin NCs showed > 80% inhibition at that same concentration (Fig. 3D).

Of the three treatment groups tested, xanthatin NCs were therefore the most potent in inhibiting spheroid formation at the tested concentrations, showing a significant reduction in cell aggregation with a consequent loss of organisation and decrease in spheroid size even at the lowest concentration tested (0.3 μM). The order of inhibitory activity was established as follows (xanthatin NCs > commercial/isolated xanthatin). Although preliminary, nanocrystallization therefore appears to significantly potentialize the pharmacological properties of xanthatin. It can be speculated that the reduced particle size of xanthatin NCs may lead to better cell internalization and possibly faster onset of action. Finally, whether nanocrystallization leads to enhanced stability in contact with the cells will require further investigation.
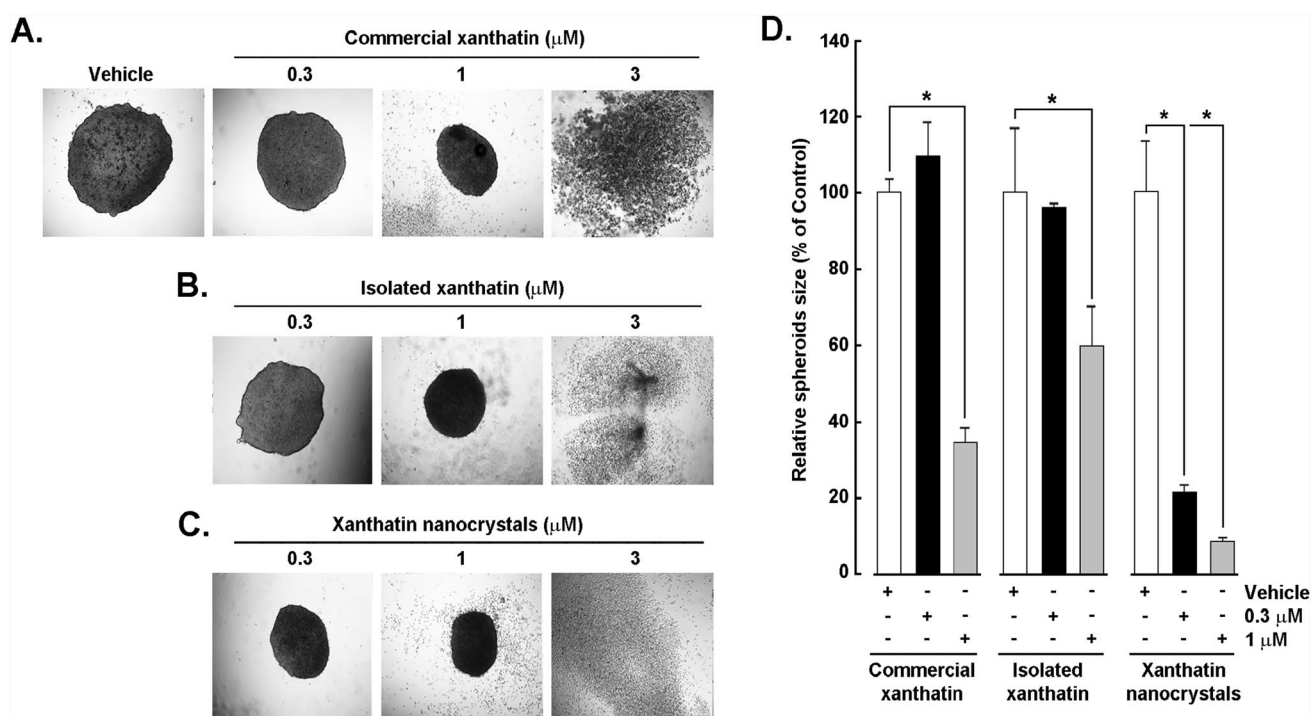
Fig. 3 Effect of commercial, isolated and nanocrystallized xanthatin on the formation of 3D HT29-derived spheroids. Monolayer HT29 cells were first cultured in complete growth media until 70–80% confluency was reached. Cells were then detached with trypsin and resuspended as 4×10^4 cells per 40 µL. Forty (40) µL cellular drops were dispensed on inverted lids of petri dishes as described in the Methods section. Phase contrast imaging was performed to assess spheroid morphological parameters after 24 h treatment with the indicated increasing concentrations of **A** commercial xanthatin, **B** isolated xanthatin, or **C** xanthatin nanocrystals. **D** Quantitative analysis of tumor spheroids area in response to commercial, isolated, or nanocrystallized xanthatin was compared to the vehicle using ImageJ software (*$p < 0.05$)

3.4 Impact of xanthatin on transcriptional regulation of transcription factors as well as immunity and inflammation related biomarkers

We next conducted a transcriptomic analysis to decipher the molecular signature of human HT29 CRC cells cultured as spheroids structures compared to that of 2D cell monolayers in order to identify signaling biomarkers which transcriptional regulation could be associated to cell invasiveness, chemoresistance, and a pro-inflammatory phenotype and whose induction could be prevented by xanthatin treatment. Spheroids were cultured for 96 h in serum-free media in the presence of 3 µM xanthatin NCs, and total RNA was extracted and transcribed to cDNA. Levels of gene expression of transcription factors related to spheroids structure formation, cancer stemness, self-renewal capacity, and invasive properties as well as inflammation biomarkers were assessed by RT² Profiler™ for Human Inflammatory Cytokines and Receptors and by Human Transcription Factors gene arrays (Fig. 4) (Table 1).

The results showed that the expression of genes encoding transcription factors involved in EMT such as *MYC*, *EGR1*, *NFKB1*, *ETS1* as well as transcription factors related to hypoxic phenotype like hypoxia-inducible factor (*HIF1A*), *ATF4*, *SP3*, *ETS1* and *FOXO1* was enriched in 3D spheroids relative to the expression of such genes in 2D (Fig. 4A). A protein–protein interaction analysis was used to assess the potential inter-relationships among the identified up-regulated (Fig. 4B, left panel) and down regulated (Fig. 4B, right panel) transcription factors as well as the identified pro-inflammatory biomarkers involved in inflammatory responses, tumor progression, angiogenesis, metastasis and tumor immunity that were also over-expressed in the 3D cellular model. These biomarkers included the C–C motif chemokine ligands 1, 2, 4, 5, 13 and 26 (CCL1, CCL2, CCL4, CCL5, CCL13, CCL26), FAS ligand (FASLG), the C-X-C motif chemokine ligands 5, 10, 11, 12 and 13 (CXCL5, CXCL10, CXCL11, CXCL12 and CXCL13), and interleukins-7, -9 and -27 (IL-7, IL-9 and IL-27) (Fig. 4C, left panel).

When the cells were treated with xanthatin NCs, the basal expression levels of the overexpressed transcription factors and inflammation markers were found to significantly decrease, as indicated by the fold change gene expression
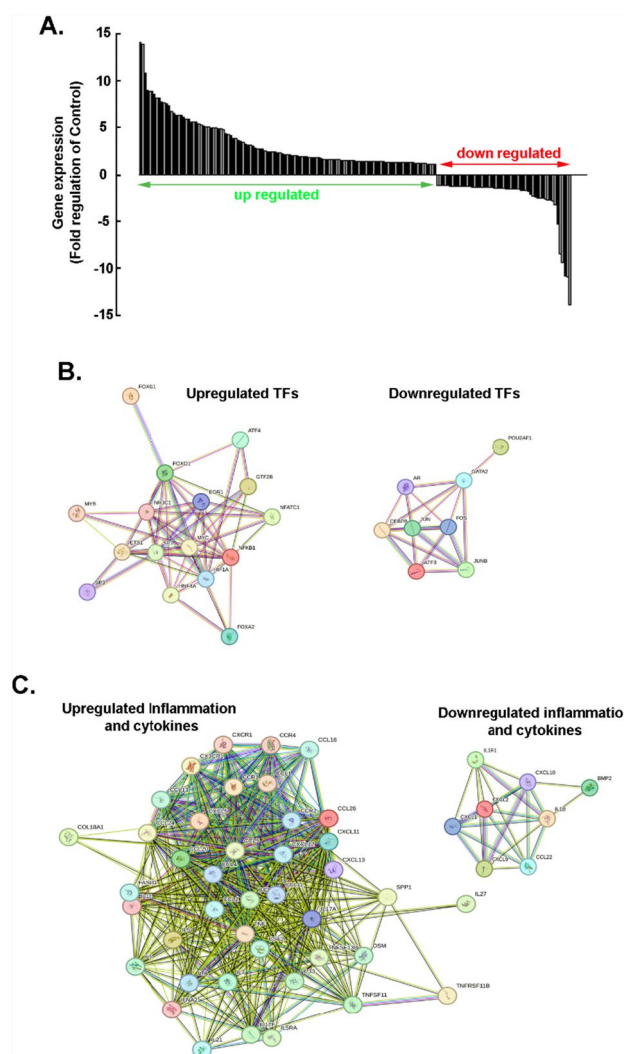
Fig. 4 Impact of xanthatin on the transcriptional regulation of transcription factors as well as immunity and inflammation related biomarkers. Human HT29 colorectal cancer cells were seeded as either two-dimensional (2D) monolayers or as three-dimensional (3D) spheroids and cultured in the absence or presence of 3 μM xanthatin nanocrystals as stated in the Methods section. Total RNA was isolated, cDNA was synthetized, and RT^2 Profiler™ PCR Array for Human Inflammatory Cytokines and Receptors (PAHS-181Z) and Human Transcription Factors (PAHS-075ZD) was performed as described in the Methods section. Gene expression of transcription factors modulated in HT29 cells showing the extent of xanthatin regulation are presented in **A** for the genes that were upregulated (top) or downregulated (bottom). A protein–protein interaction network analysis of differentially expressed genes of transcription factors **B** and inflammatory markers **C** was constructed by STRING as described in the Methods section. Every node corresponds to a protein and every edge corresponds to a protein–protein interaction

variation compared to 2D control cells, suggesting that the xanthatin molecule could regulate a specific subset of genes whose protein product influences cancer cell molecular signature related to angiogenesis, inflammatory responses as well as to cell survival.

3.5 Time-course inhibition of the TNFα induced phospho-ERK and phospho-IκB expression in HT29 cells by commercial xanthatin

There is clear evidence showing a connection between inflammatory processes and EMT, both of which are linked to tumor aggressiveness and poor clinical outcomes. For instance, the inflammatory cytokine TNFα has been shown to induce EMT in tumor cells and to promote invasion by activating the nuclear factor kappa-B (NFκB) pathway. Additionally, chemotactic factors like IL-8 play a role in the EMT process by activating signaling pathways such as ERK, JAK2/STAT3, and phosphoinositide 3-kinase (PI3K)/ protein kinase B (AKT). Prolonged activation of ERK signaling has been associated with several negative

Table 1 Influence of xanthatin treatment on the expression level of inflammatory genes and transcription factors related to cancer invasiveness, progression, angiogenesis, metastasis and tumor immunity

Upregulated gene	Function
ATF4	Upregulated during EMT and plays a critical role in cellular stress responses and metabolic adaptation. It is upregulated under hypoxic conditions and plays a role in cellular stress responses, including autophagy and metabolic adaptation
HIF1A	A key regulator of cellular responses to hypoxia, driving angiogenesis, metabolic adaptation, immune regulation, and promoting epithelial to mesenchymal transition
FOXG1	Promotes EMT in hepatocellular carcinoma by activating the Wnt signaling pathway
NFATC1	Promotes increased colon cancer cell invasion and metastasis under hypoxic conditions
NF-kB1	Plays a significant role in hypoxia-induced inflammatory responses and cancer progression
HNF4A	Plays a significant role in EMT through inflammatory signaling pathways and it is also involved in metabolic regulation and can influence cancer cell behavior under hypoxic condition
CCL11	Known for recruiting immune cells to the tumor microenvironment (TME), has an unclear role in the context of its expression, patient prognosis, and the presence of tumor-infiltrating immune cells
CCL13	Key chemotactic factors, which play crucial roles in cancer cell biology, playing a significant part in modulating the tumor microenvironment (TME), influencing tumor progression, metastasis, and immune responses
CCL16	Chemotactic factor belonging to the α-chemokine subfamily. It plays a significant role in the progression of cancer, as well as the course of atherosclerosis, renal fibrosis, and non-alcoholic fatty liver disease (NAFLD)
CCL24	Contributes to tumorigenesis as well as inflammatory diseases like asthma and allergies and its used as a potential biomarker in several cancers including colon cancer, non-small cell cancer, and nasopharyngeal carcinoma
CCL2	Frequently overexpressed in cancer cells and other cells in the tumor microenvironment. Its levels are associated with more aggressive malignancies, a higher probability of metastasis, and poorer outcomes in a wide range of cancers
CCL20	CCL20-CCR6 axis promotes cancer progression directly by enhancing migration and proliferation of cancer cells and indirectly by remodeling the tumor microenvironment through immune cell control
CCR1	Involved in the recruitment of inflammatory cells to the tumor microenvironment, which can contribute to the promotion of metastasis. Chemokines like CCL3-CCR1 can enhance tumor cell migration and invasion by promoting the movement of immune cells that facilitate tissue remodeling and angiogenesis
CCR2	Plays a critical role in the establishment of an inflammatory microenvironment that supports tumor progression. Its presence in the tumor can enhance cancer cell migration and invasion, contributing to metastasis
FASLG	Plays a significant role in cancer biology by influencing tumor progression, immune evasion, and treatment responses. Tumor cells with FASL expression can then induce cell death of these immune cells, reducing the effectiveness of the immune system in recognizing and eliminating the tumor

The top 15 genes identified as upregulated in 3D spheroids, compared to their expression levels in 2D monolayers, and that were successfully targeted by xanthatin. The assessment of transcriptional regulation was conducted using RT^2 Profiler™ gene arrays for Human Inflammatory Cytokines and receptors, and Transcription Factors

outcomes in cancer patients, including cell transformation, metastasis, resistance to anticancer drugs, and poor prognosis, which aligns with its established role in EMT induction [24–26]. Considering the evidence gathered from the above experiments, we went on to investigate the time-resolved dissection of early proteome and phosphoproteome changes in response to TNFα induction and to xanthatin treatment (Fig. 5).

For this, serum-starved cells were treated with 1 µM commercial xanthatin for 24 h and were next stimulated with 30 ng/mL TNFα for the indicated times (Fig. 5A). Proteins were extracted as described in the Methods section and Western blot analysis was performed to assess the extent of total ERK, phospho-ERK, total IκB and phospho-IκB expression. As shown in the Fig. 5B, maximal phosphorylation of IκB appears by 5 min after TNFα treatment of HT29 cells. However, the phosphorylation level of IκB decreased during the rest of the experiment. On the other hand, activation of ERK by TNFα reached its peaked after 30 min of stimulation and declined thereafter at 60 min. Densitometric analysis of the phosphorylation status of phospho ERK/ERK (left panel) and phospho IκB/IκB (right panel) in HT29-treated cells with 1 µM commercial xanthatin shows the quantitative extent of ERK inactivation and prevention of IκB degradation induced by the treatment with the molecule.

Fig. 5 Time-course inhibition of the TNFα induced phospho-ERK and phospho-IκB expression in HT29 cells by commercial xanthatin. Serum-starved cells were treated with commercial xanthatin (1 μM) for 24 h. Cells were next stimulated with 30 ng/mL TNFα for the indicated times and proteins extracted as described in the Methods section. **A** Western Blot analysis was performed to assess the extent of total ERK, phospho-ERK, total IκB and phospho-IκB expression as described in the Methods Section. **B** Scanning densitometry analysis of the phosphorylation status of phospho ERK/ERK (left panel) and phospho IκB/IκB (right) in HT29 treated cells with 1 μM commercial xanthatin
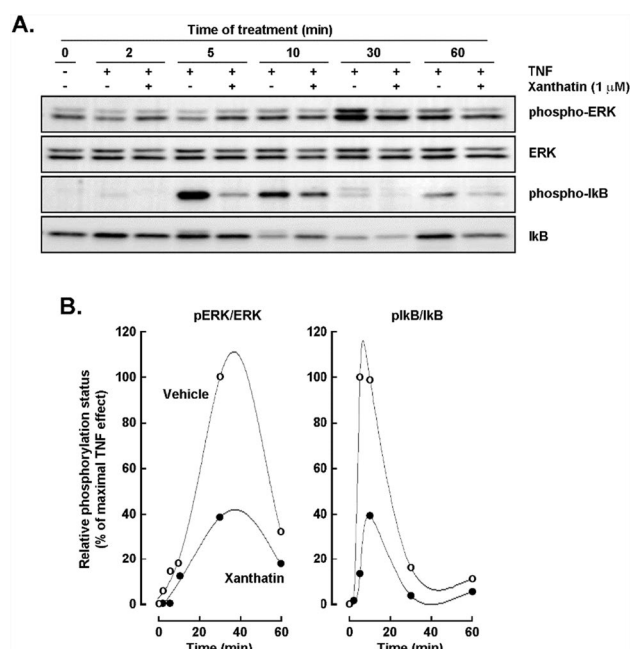
3.6 Inhibition of the TNFα-induced phosphorylation of ERK and of IκB expression in HT29 cells by commercial xanthatin, isolated xanthatin or xanthatin nanocrystals

Having previously demonstrated the effect of xanthatin on the temporal expression of phosphorylated markers such as ERK and IκB, we next proceeded to evaluate the effect of commercial xanthatin, isolated xanthatin and xanthatin NCs, to compare the efficacy of each treatment (Fig. 6).

For this purpose, HT29 cells were treated with 30 ng/mL TNFα in the presence or absence of 0.3 μM of commercial xanthatin, isolated xanthatin or xanthatin NCs in serum-free media for 30 min (phospho-ERK/ERK) or for 5 min (phospho-IκB/IκB) and immunoblotting analysis was performed as described in the Methods section. As shown in the figure, phosphorylation status of ERK and IκB proteins triggered by TNFα stimulation was efficiently reduced after xanthatin treatment (Fig. 6A). Interestingly, densitometric analysis revealed that treatment with commercial xanthatin was less effective in reducing the phosphorylation status for both proteins when the cells were co-treated with TNFα and commercial xanthatin. In addition, there were no relevant differences in the effect observed after treatment with the isolated xanthatin and NCs, both of which proved to be similarly efficient in preventing phosphorylation of ERK and IκB (Fig. 6B). Transcript levels of TNFα-induced COX-2 and IL-1B were also found to be repressed efficiently by isolated xanthatin and xanthatin NCs (Fig. 6C). Collectively, xanthatin is already considered a kinase inhibitor since it has been identified as an inhibitor of VEGFR2 (vascular endothelial growth factor receptor 2) signaling, which plays a crucial role in angiogenesis and tumor growth [27], and has shown inhibitory effects on GSK3β (glycogen synthase kinase 3 beta), which is involved in various cellular processes, including cell proliferation and survival [28]. These properties confirm xanthatin, and its nanocrystallized form, a promising compound for cancer research, in part through targeting tumor angiogenesis and growth.

3.7 Xanthatin inhibits the induction of mediators expressed in the acquisition of hypoxic, inflammatory and EMT phenotypes in 3D colorectal cancer spheroids

A hypoxic inflammatory TME as well as TME-induced EMT contribute to cancer progression and invasiveness [29]. Reduced oxygenation leads to induction of several hypoxia-responsive genes. The primary mediating factor is HIF1A which stimulates the expression of a variety of cytokines from inflammatory cells, and whose target genes include erythropoietin, vascular endothelial growth factor (VEGF), glucose transporter-1 (Glut-1), as well as the direct up regulation of COX-2 expression and increasing of Prostaglandin E2 (PGE2) production which leads to activation of

Fig. 6 Inhibition of the TNFα-induced phosphorylation of ERK and of IκB expression in HT29 cells by commercial xanthatin, isolated xanthatin or xanthatin nanocrystals. **A** HT29 cells were treated with 30 ng/mL TNFα in the presence or absence of 0.3 μM of commercial xanthatin, isolated xanthatin, or xanthatin nanocrystals in serum-free media for 30 min (phospho-ERK/ERK) or for 5 min (phospho-IκB/IκB). Immunoblotting analysis was performed as described in the Methods section. **B** Scanning densitometry data of phospho-ERK/ERK (left panel) and phospho-IκB/IκB (right panel) in HT29 cells treated with 0.3 μM commercial xanthatin, isolated xanthatin or xanthatin nanocrystals. **C** Total RNA was extracted and RT-qPCR performed as described in the Methods section for *COX-2* and *TNFα* expression
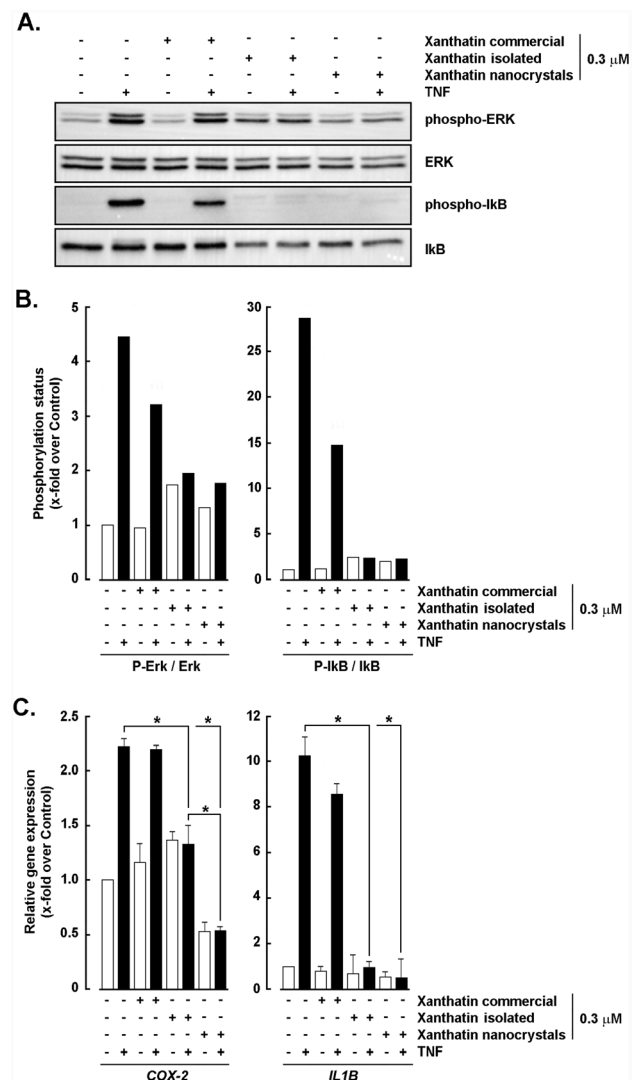
the Ras-MAPK pathway promoting tumour maintenance, survival and progression [30]. Under hypoxic conditions, yes-associated protein 1 (YAP1), a well-established oncogene that binds to transcriptional enhanced associate domain (TEAD) protein family, contributes to the induction of EMT, promoting the transcription of genes that enhances the loss of epithelial characteristics and the acquisition of mesenchymal characteristics [31]. For example, YAP1-TEAD activates the expression of transcription factors such as Snail, Twist, and ZEB1, which are known to repress the expression of epithelial proteins such as E-cadherin and promote the expression of mesenchymal proteins such as Vimentin and N-cadherin [32]. The YAP1-TEAD also regulates the expression of proangiogenic genes, such as VEGF, which promotes the formation of new blood vessels and helps tumour cells obtain the nutrients necessary for their growth and expansion, contributing to the metabolic reprogramming of tumour cells, promoting aerobic glycolysis, along with the up-regulation of the expression of glucose transporters at transcriptional level to promote cell glycolysis [29, 30].

Given that xanthatin was previously documented to alter the expression of cellular markers related to hypoxic conditions, inflammation, as well as the acquisition of a mesenchymal phenotype in our cellular model, we went on to further investigate the impact of our treatments on the molecular signature of colorectal spheroids considering the following biomarkers: COX-2, GLUT1, VEGF, HIF1, YAP1 and TEAD. Spheroids were generated from adherent human HT29 colorectal cancer cell monolayer cultures as described in the Methods section. Total RNA was extracted, and RT-qPCR was performed to assess gene expression levels. *COX-2*, *GLUT1*, *VEGF* and *HIF1* were all significantly up-regulated upon spheroid formation when compared to cell monolayers (Fig. 7), supporting the formation of a hypoxic environment within the spheroids.

Xanthatin treatments were found to efficiently inhibit all these induced genes involved in spheroids formation, where xanthatin NCs proved to be the most effective, returning the levels of expression to a value close to the monolayers
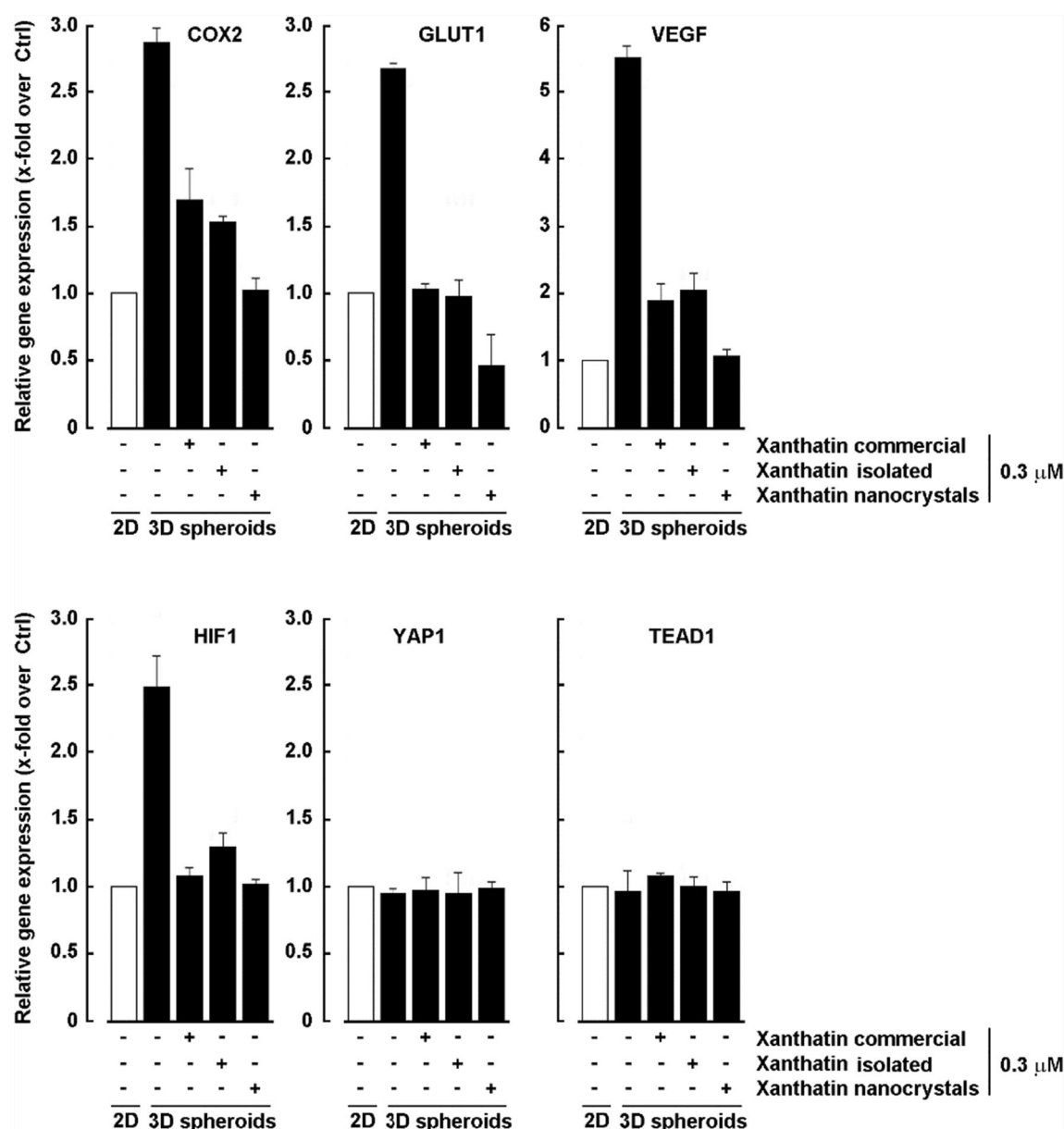
Fig. 7 Inhibition of the induction of mediators expressed in the acquisition of hypoxic, inflammatory, and EMT phenotype in colorectal cancer tumorspheres. Tumorspheres were generated from human HT29 colorectal cancer cell monolayer cultures as described in the Methods section and were treated in the absence or presence of 0.3 μM of commercial xanthatin, isolated xanthatin and nanocrystals. RT-qPCR was performed to assess the gene expression levels of *COX-2*, *GLUT1*, *VEGF*, *HIF-1*, *YAP1* and *TEAD* in either HT29 monolayers (white bars) or tumorspheres (black bars). Protein expression levels of COX-2 were previously assessed in adherent monolayers by immunoblotting

baseline. Interestingly, YAP1 and TEAD expression were not found to be overexpressed in the spheroids compared to the monolayers and xanthatin treatment did not alter their expression in any case.

3.8 Xanthatin inhibits TNFα-induced migration of HT29 cells

Finally, a real-time cell migration assay was performed to assess HT29 cells' chemotactic response to increasing concentrations of commercial xanthatin, isolated xanthatin and NCs (Fig. 8). For this, HT29 cells were co-treated with the pro-inflammatory cytokine TNFα, to stimulate migration, and with 0.1, 0.3, 1 and 3 μM of commercial xanthatin, isolated xanthatin and NCs.
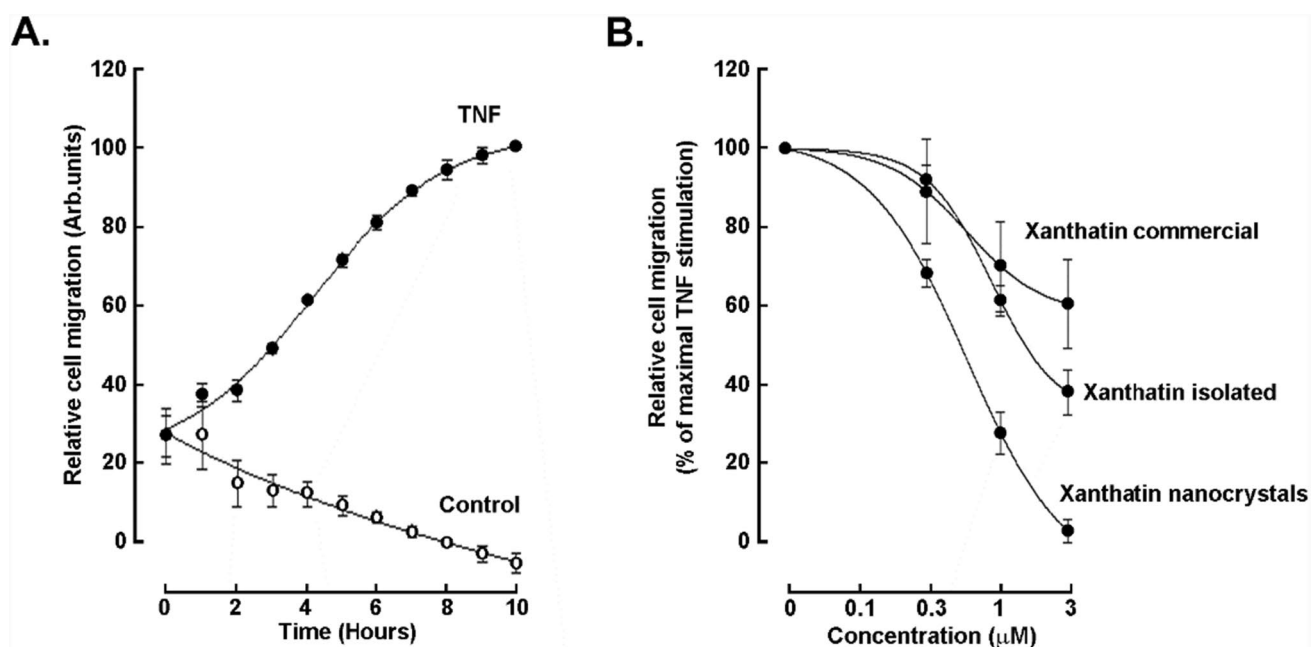
Fig. 8 Xanthatin inhibits TNFα-induced migration of HT29 cells. A real time chemotactic cell migration assay was conducted as described in the Methods section. To assess the impact of xanthatin treatments upon TNFα-stimulated HT29 cells, chemotaxis was monitored in response to **A** Control (serum free media) or 30 ng/mL TNFα 30 ng/mL, or **B** the indicated increasing concentrations of commercial xanthatin, isolated xanthatin, or xanthatin nanocrystals. The results are expressed as the percent of maximal stimulation induced by TNFα

As shown in the figure, cell migration was efficiently induced by TNFα (Fig. 8A) compared to unstimulated cells, whose migration pattern was found uninduced. We further found that xanthatin dose-dependently inhibited TNFα-stimulated migration for all three treatments, however, the NCs proved to be significantly more potent with a marked inhibitory effect at only 0.3 μM when compared to commercial or isolated xanthatin, and almost completely inhibiting cell migration when the concentration was 3 μM (Fig. 8).

4 Discussion

Previous studies involving xanthatin demonstrated that this molecule inhibits cancer cell proliferation, triggers caspase-dependent apoptosis, and induces cell cycle arrest [24, 33, 34]. The anti-inflammatory effects of xanthatin are however not yet fully understood. Here, we developed an inflammation model using the HT29 CRC cell line to investigate the inflammation-suppressive functions of xanthatin, along with its potential mechanisms in targeting signaling pathways. Additionally, we aimed to demonstrate the potential pharmacological advantages of nanocrystallization as a strategy to enhance biological activity and ultimately improve future in vivo xanthatin bioavailability and biological efficacy. To achieve this preliminary pharmacological study, we assessed the molecular and cellular effects of xanthatin and of its crystalline form in 2D and 3D in vitro cell models.

Tumor cell growth is marked by several key features: the continuous activation of pathways that promote cell proliferation, resistance to cell death, the acquisition of replicative immortality, and reprogramming of their metabolic processes [35, 36]. In this adaptive context, analysis of chemotherapeutic drugs potency represents a fundamental aspect of pre-clinical pharmacology [35, 37, 38]. The first step of our study consisted in defining the cytotoxic spectrum of xanthatin and the potency of xanthatin NCs on the reduction of HT29 cellular viability in vitro. Our data showed that xanthatin treatment decreased the viability of 2D HT29 monolayer cells with xanthatin NCs displaying the highest inhibition rate. Once xanthatin cytotoxicity in the 2D cellular culture assessed, we went further to measure the impact of our molecules in the 3D tumorspheres formation compared to the 2D monolayer cultures. Tumour spheroids are a well-characterised 3D culture system that, better than 2D monolayers, mimics the physiological tissue organisation and complexity of solid tumours with a hypoxic core [39]. Morphological changes in response to effective anticancer drug treatment in 3D tumour spheroids, such as reduced spheroid size, loss of spheroid compactness and integrity or smooth

surface, are considered highly reliable [40, 41]. Here, we observed a reduction in the tumorspheres size and sphericity as well as a loss of compactness and integrity according to the concentrations of xanthatin tested, with xanthatin NCs being the most effective one.

The tumor-promoting inflammatory microenvironment is characterized by heterogeneous inflammatory cellular components that produce growth-stimulating mediators, including inflammatory cytokines [31, 41], growth factors, chemokines, genotoxic substances, and factors that induce DNA damage [32]. In this study, we then examined the cellular inflammatory response induced in HT29 3D spheroid cells to uncover the molecular signature of these cancer cells. Our goal was to identify biomarkers that could potentially be targeted effectively by our molecules of interest. First, we showed that xanthatin treatment inhibited the TNFα-induced expression of COX-2, a crucial inflammatory enzyme primarily responsible for the synthesis of PGE2 [29, 31, 35], at both the gene and protein levels. COX-2 expression also promotes cancer stem cell (CSC)-like activity, and its inhibition may further reduce resistance to apoptosis, proliferation, angiogenesis, invasion, and metastasis in cancer cells [42]. As cancer-related inflammation and epithelial-to-mesenchymal transition (EMT) are closely interconnected processes [43, 44], we further explored whether cancer cells undergoing EMT can produce pro-inflammatory factors, creating a feedback loop that would sustain inflammation and further promote EMT.

Here, multiple factors have been identified to be implicated in EMT including transcription factors such as SNAIL, TWIST, ZEB, PRRX1, FOXC2, GATA, downregulation of epithelial cell markers such as E-cadherin, and upregulation of mesenchymal markers such as of N-cadherin, vimentin, fibronectin, various matrix metalloproteases (MMPs), and β1 and β3 integrins [29, 45]. Through the hypoxic core provided by our 3D spheroids cell model, we further show the crosstalk between the promoted EMT and 3D spheroids hypoxic core [46]. Such modulation of the cellular landscape requires the hypoxia-inducible factors (HIFs) to orchestrate the transcriptional responses under the hypoxic environment [47]. HIF1α activates the transcription of factors such as VEGF, angiopoietin 2 (ANGPT2), stromal-derived factor 1, COX-2 and stem cell factors (SCF) [48]. Some oncogenes further cooperate with HIF1α to increase its stabilization and transcriptional activity [49], subsequently promoting the transcription of genes associated to the acquisition of mesenchymal characteristics [50]. Among these oncogenes is the Yes-associated protein (YAP), a transcriptional activator that interacts with TEAD transcription factors [51, 52], stimulating the upregulation of multiple genes that promote angiogenesis, vascularization, tumor growth, metabolic reprogramming, and the acquisition of an invasive phenotype [53–55]. As inflammation mediators can alter the TME, manipulating or neutralizing abnormal cytokines in the TME by xanthatin may represent a promising strategy for cancer therapy [41]. Cytokines such as EGF, FGF, and IL-6 promote the proliferation and survival of tumor cells. Others, like TGFβ, IL-1, IL-6, IL-8, and TNFα, contribute to the EMT and maintenance of stemness in tumor cells, facilitating a more invasive phenotype [56]. While the potential long-term anti-inflammatory and anticancer effects of xanthatin NCs and bioavailability will require to be confirmed in follow-up in vivo studies, a recent study on dapsone, an anti-inflammatory drug, demonstrated that nanocrystallization significantly improved its solubility, dissolution, and preserved in vitro anti-inflammatory activity [57]. Nanocrystallization offers therefore alongside a promising approach to also enhancing the xanthatin pharmacological properties of anticancer drugs [58].

Chemokines also play an important role in the progression of cancers [59], promoting tumor growth, senescence, angiogenesis, EMT, metastasis and immune evasion [60, 61]. The NF-kappa B family of transcription factors regulates the expression of numerous chemokines and facilitates the secretion of chemokines that bind to CXCR2, as well as IL-6 [62]. Additionally, the chemokine CXCL8 and its receptor CXCR1 are significantly upregulated in cells undergoing EMT. Chemokines such as CXCL1, CXCL2, CXCL3, and CXCL12 enhance tumor cell proliferation by activating the MAPK/ERK signaling pathway [60]. Chemokine receptor 4 (CXCR4) is one of the early identified hypoxia/HIF1α target genes that mediates hypoxia-induced angiogenesis and metastasis [50, 61]. Here, we examined the transcriptional regulation of transcription factors as well as inflammation related markers in human HT29 CRC cells cultured as 3D spheroids were compared to that of 2D cell monolayers to identify signaling biomarkers associated to cell invasiveness, chemoresistance, and to a pro-inflammatory phenotype and whose transcriptional regulation could be prevented by xanthatin treatment. We found that HT29 3D spheroids over-expressed markers involved in EMT transition comprising MYC, EGR1, NFKB1, ETS1; hypoxic status such as HIF1A, ATF4, SP3, ETS1 and FOXO1; and inflammation including IL-7, IL-9, IL-27, CCL1, CCL2, CCL4, CCL5, CXCL5, CXCL10 and CXCL11. Xanthatin NCs efficiently decreased this basal overexpression indicating the potential role of the molecule in targeting the acquired mesenchymal and inflammatory phenotype of HT29 CRC cells.

Two major pathways that are frequently mutated in various human cancers, including CRC, are the Ras-MAPK and PI3K/AKT signaling pathways, and their activation stimulates cell growth, proliferation, and survival [42, 59]. Interestingly, recent studies suggest that the COX-2/PGE2 pathway may modify apoptotic thresholds and promote pro-survival mechanisms by engaging the PI3K/AKT pathway [63], ERK signalling, cyclic adenosine monophosphate (cAMP)/protein kinase A signalling and activation of epidermal growth factor receptor (EGFR) signalling [64]. TNFα induction of EMT in

tumor cells and invasion is mediated through the activation of the NFκB and AKT signaling pathways [65], and often converge to regulators such as ERK and PI3K/Akt [66]. In fact, sustained activation of ERK signaling is linked to cell transformation, resistance to anticancer drugs, and poor prognosis in cancer, [63]. In our research, we aimed to decipher the early changes in the proteome and phosphoproteome of HT29 cells in response to TNFα by assessing the levels of total ERK, phosphorylated ERK, total IκB, and phosphorylated IκB. Initially, we observed that the expression levels of the phosphoproteins significantly changed over time, and was significantly reduced following treatment with xanthatin. Notably, there were no substantial differences in the outcomes observed after treatment with isolated xanthatin and NCs, as both displayed similar levels of activity in preventing the phosphorylation of ERK and IκB.

For cancer to spread throughout the body, cancer cells must undergo several processes: they need to migrate and invade the extracellular matrix (ECM), enter the bloodstream (a process known as intravasation), attach to distant sites, and finally exit the bloodstream (extravasation) to form new tumors [67]. Here we observed that HT29 cells by themselves did not demonstrate significant basal migration, while it was significantly induced in response to TNFα stimulation. This inflammatory cytokine-induced migration pattern was efficiently targeted by xanthatin in a dose-dependent manner with NCs being the most powerful when compared to commercial or isolated xanthatin.

Study limitations must be acknowledged. Although 3D cell culture models have advanced our understanding of cancer biology, they still face several limitations, particularly in the context of chemoresistance and the complexity of the TME. Aspects include (1) Incomplete replication of TME, as 3D cell models still fall short of fully replicating the complexity of in vivo environments; (2) Tumor heterogeneity issues, as tumors are highly heterogeneous, with significant variations in cell types, genetic mutations, and microenvironments within the same tumor. Therefore, 3D models, including organoids, may not capture this heterogeneity adequately in vitro; (3) Chemoresistance mechanisms, although 3D models provide a better platform for studying chemoresistance than 2D models, eventual issues with xanthatin diffusion in 3D models could lead to variable drug exposure and resistance patterns that may not accurately reflect future in vivo conditions. In vitro models are also generally less suitable for long-term studies due to issues like cell viability and changes in cell behavior over time. Despite these limitations, our 3D spheroid models remain a valuable tool for cancer research, providing pre-clinical molecular insights that are not possible with traditional 2D cultures. They are particularly useful for initial screenings and mechanistic studies on xanthatin NCs, eventually complementing in vivo research.

5 Conclusions

In this study, we evaluated the efficacy of nanocrystallisation and mechanism of action of xanthatin using both 2D and 3D inflammation models established after TNFα stimulation. Our findings provide new insights into the antitumor properties of xanthatin through efficiently targeting key biomarkers associated with EMT, hypoxia, inflammation, and migration. In our models, xanthatin NCs were shown to reduce the overexpression of COX-2 protein and to inhibit the expression of phosphorylated proteins such as IκBα and ERK1/2, as well as inflammatory cytokines, related receptors, and transcription factors that play significant roles in processes like the acquisition of an invasive phenotype, proliferation, migration, and metastasis. The observed changes suggest that xanthatin's antitumor mechanisms may be mediated through the inhibition of the NFκB and MAPK pathways. Among the three treatment approaches tested, xanthatin NCs proved to be the most effective. Finally, our findings indicate that the use of nanocrystallisation as a valuable platform to successfully enhance the physicochemical properties of poorly soluble drugs ultimately led to improved effectiveness and a greater pharmacological effect of our target molecule.

Declarations

Ethics and consent to participate Not applicable.

Consent for publication Not applicable.

Competing interests The authors declare no potential conflicts of interest with respect to the research, authorship, and/or publication of this article.

References

1. Wang M, Chen S, He X, Yuan Y, Wei X. Targeting inflammation as cancer therapy. J Hematol Oncol. 2024;17(1):13. https://doi.org/10.1186/s13045-024-01528-7. (**PMID: 38520006 PMCID: PMC10960486**).
2. Zhang S, Xiao X, Yi Y, Wang X, Zhu L, Shen Y, Lin D, Wu C. Tumor initiation and early tumorigenesis: molecular mechanisms and interventional targets. Signal Transduct Target Ther. 2024;9(1):149. https://doi.org/10.1038/s41392-024-01848-7. (**PMID: 38890350 PMCID: PMC11189549**).
3. Hou J, Karin M, Sun B. Targeting cancer-promoting inflammation—have anti-inflammatory therapies come of age? Nat Rev Clin Oncol. 2021;18(5):261–79. https://doi.org/10.1038/s41571-020-00459-9. (**Epub 2021 Jan 19 PMID: 33469195 PMCID: PMC8978805**).
4. Zhao H, Wu L, Yan G, Chen Y, Zhou M, Wu Y, Li Y. Inflammation and tumor progression: signaling pathways and targeted intervention. Signal Transduct Target Ther. 2021;6(1):263. https://doi.org/10.1038/s41392-021-00658-5. (**PMID: 34248142 PMCID: PMC8273155**).
5. Roncati L, Figueiredo CR. Editorial: hallmark of cancer: tumor promoting inflammation. Front Oncol. 2023;7(13):1242407. https://doi.org/10.3389/fonc.2023.1242407. (**PMID: 37483513 PMCID: PMC10361747**).
6. Greten FR, Grivennikov SI. Inflammation and cancer: triggers, mechanisms, and consequences. Immunity. 2019;51(1):27–41. https://doi.org/10.1016/j.immuni.2019.06.025. (**PMID: 31315034 PMCID: PMC6831096**).
7. Khalyfa AA, Punatar S, Aslam R, Yarbrough A. Exploring the inflammatory pathogenesis of colorectal cancer. Diseases. 2021;9(4):79. https://doi.org/10.3390/diseases9040079. (**PMID: 34842660 PMCID: PMC8628792**).
8. Li Q, Geng S, Luo H, Wang W, Mo YQ, Luo Q, Wang L, Song GB, Sheng JP, Xu B. Signaling pathways involved in colorectal cancer: pathogenesis and targeted therapy. Signal Transduct Target Ther. 2024;9(1):266. https://doi.org/10.1038/s41392-024-01953-7. (**PMID: 39370455 PMCID: PMC11456611**).
9. Hanahan D, Weinberg RA. Hallmarks of cancer: the next generation. Cell. 2011;144(5):646–74. https://doi.org/10.1016/j.cell.2011.02.013. (**PMID: 21376230**).
10. Wood LD, Parsons DW, Jones S, Lin J, Sjöblom T, Leary RJ, Shen D, Boca SM, Barber T, Ptak J, Silliman N, Szabo S, Dezso Z, Ustyanksky V, Nikolskaya T, Nikolsky Y, Karchin R, Wilson PA, Kaminker JS, Zhang Z, Croshaw R, Willis J, Dawson D, Shipitsin M, Willson JK, Sukumar S, Polyak K, Park BH, Pethiyagoda CL, Pant PV, Ballinger DG, Sparks AB, Hartigan J, Smith DR, Suh E, Papadopoulos N, Buckhaults P, Markowitz SD, Parmigiani G, Kinzler KW, Velculescu VE, Vogelstein B. The genomic landscapes of human breast and colorectal cancers. Science. 2007;318(5853):1108–13. https://doi.org/10.1126/science.1145720. (**Epub 2007 Oct 11 PMID: 17932254**).
11. Sülsen VP. Sesquiterpene lactones and diterpenes: promising therapeutic candidates for infectious diseases, neoplasms and other chronic disorders. Molecules. 2021;26(5):1251. https://doi.org/10.3390/molecules26051251. (**PMID: 33652593 PMCID: PMC7956199**).
12. Dhyani P, Sati P, Sharma E, Attri DC, Bahukhandi A, Tynybekov B, Szopa A, Sharifi-Rad J, Calina D, Suleria HAR, Cho WC. Sesquiterpenoid lactones as potential anti-cancer agents: an update on molecular mechanisms and recent studies. Cancer Cell Int. 2022;22(1):305. https://doi.org/10.1186/s12935-022-02721-9. (**PMID: 36207736 PMCID: PMC9540722**).
13. Paço A, Brás T, Santos JO, Sampaio P, Gomes AC, Duarte MF. Anti-inflammatory and immunoregulatory action of sesquiterpene lactones. Molecules. 2022;27(3):1142. https://doi.org/10.3390/molecules27031142. (**PMID: 35164406 PMCID: PMC8839508**).
14. Matos MS, Anastácio JD, Nunes Dos Santos C. Sesquiterpene lactones: promising natural compounds to fight inflammation. Pharmaceutics. 2021;13(7):991. https://doi.org/10.3390/pharmaceutics13070991.
15. Padilla-Gonzalez GF, dos Santos FA, Da Costa FB. Sesquiterpene lactones: more than protective plant compounds with high toxicity. Crit Rev Plant Sci. 2016;35(1):18–37. https://doi.org/10.1080/07352689.2016.1145956.
16. Zhang J, Zhao R, Jin L, Pan L, Lei D. Xanthanolides in Xanthium L.: structures synthesis and bioactivity. Molecules. 2022;27(23):8136. https://doi.org/10.3390/molecules27238136. (**PMID: 36500229 PMCID: PMC9735877**).
17. Moujir L, Callies O, Sousa PMC, Sharopov F, Seca AML. Applications of sesquiterpene lactones: a review of some potential success cases. Appl Sci. 2020;10:3001. https://doi.org/10.3390/app10093001.
18. Li WD, Wu Y, Zhang L, Yan LG, Yin FZ, Ruan JS, Chen ZP, Yang GM, Yan CP, Zhao D, Lu Y, Cai BC. Characterization of xanthatin: anticancer properties and mechanisms of inhibited murine melanoma in vitro and in vivo. Phytomedicine. 2013;20(10):865–73. https://doi.org/10.1016/j.phymed.2013.03.006. (**Epub 2013 May 7 PMID: 23664560**).

19. Tao L, Sheng X, Zhang L, Li W, Wei Z, Zhu P, Zhang F, Wang A, Woodgett JR, Lu Y. Xanthatin anti-tumor cytotoxicity is mediated via glycogen synthase kinase-3β and β-catenin. Biochem Pharmacol. 2016;1(115):18–27. https://doi.org/10.1016/j.bcp.2016.06.009. (**Epub 2016 Jun 16 PMID: 27321043**).

20. Jarvis M, Krishnan V, Mitragotri S. Nanocrystals: a perspective on translational research and clinical studies. Bioeng Transl Med. 2018;4(1):5–16. https://doi.org/10.1002/btm2.10122. (**PMID: 30680314 PMCID: PMC6336669**).

21. Khosrawipour T, Schubert J, Kulas J, Migdal P, Arafkas M, Bania J, Khosrawipour V. Creating nanocrystallized chemotherapy: the differences in pressurized aerosol chemotherapy (PAC) via intracavitary (IAG) and extracavitary aerosol generation (EAG) regarding particle generation, morphology and structure. J Cancer. 2020;11(6):1308–14. https://doi.org/10.7150/jca.39097. (**PMID: 32047537 PMCID: PMC6995397**).

22. Jahangir MA, Imam SS, Muheem A, et al. Nanocrystals: characterization overview, applications in drug delivery, and their toxicity concerns. J Pharm Innov. 2022;17:237–48. https://doi.org/10.1007/s12247-020-09499-1.

23. Ferrer JP, Zampini IC, Cuello AS, Francisco M, Romero A, Valdivia D, Gonzalez M, Salas C, Lamar AS, Isla MI. Cytotoxic compounds from aerial organs of *Xanthium strumarium*. Nat Prod Commun. 2016;11(3):371–4 (**PMID: 27169184**).

24. Piloto-Ferrer J, Sánchez-Lamar Á, Francisco M, González ML, Merino N, Aparicio G, Pérez C, Rodeiro I, Lopes MTP. *Xanthium strumarium´s* xanthatins induces mitotic arrest and apoptosis in CT26WT colon carcinoma cells. Phytomedicine. 2019;57:236–44. https://doi.org/10.1016/j.phymed.2018.12.019. (**Epub 2018 Dec 17 PMID: 30797985**).

25. Alpízar-Pedraza D, Veulens AN, Ginarte YMÁ, Piloto-Ferrer J, Sánchez-Lamar Á. Xanthatin and 8-epi-xanthatin as new potential colchicine binding site inhibitors: a computational study. J Mol Model. 2023;29(2):36. https://doi.org/10.1007/s00894-022-05428-w. (**PMID: 36627468**).

26. Rasouli M, Safari F, Kanani MH, Ahvati H. Principles of hanging drop method (Spheroid Formation) in cell culture. Methods Mol Biol. 2024. https://doi.org/10.1007/7651_2024_527. (**PMID: 38411887**).

27. Yu Y, Yu J, Pei CG, Li YY, Tu P, Gao GP, Shao Y. Xanthatin, a novel potent inhibitor of VEGFR2 signaling, inhibits angiogenesis and tumor growth in breast cancer cells. Int J Clin Exp Pathol. 2015;8(9):10355–64 (**PMID: 26617743 PMCID: PMC4637558**).

28. Tao L, Fan F, Liu Y, Li W, Zhang L, Ruan J, Shen C, Sheng X, Zhu Z, Wang A, Chen W, Huang S, Lu Y. Concerted suppression of STAT3 and GSK3β is involved in growth inhibition of non-small cell lung cancer by Xanthatin. PLoS ONE. 2013;8(11): e81945. https://doi.org/10.1371/journal.pone.0081945. (**PMID: 24312384 PMCID: PMC3842975**).

29. Liu W, Shen SM, Zhao XY, Chen GQ. Targeted genes and interacting proteins of hypoxia inducible factor-1. Int J Biochem Mol Biol. 2012;3(2):165–78 (**Epub 2012 May 31 PMID: 22773957 PMCID: PMC3388736**).

30. Yan L, Cai Q, Xu Y. Hypoxic conditions differentially regulate TAZ and YAP in cancer cells. Arch Biochem Biophys. 2014;15(562):31–6. https://doi.org/10.1016/j.abb.2014.07.024. (**Epub 2014 Jul 29 PMID: 25078107 PMCID: PMC4197065**).

31. Zhao L, Wu Y, Xu Z, Wang H, Zhao Z, Li Y, Yang P, Wei X. Involvement of COX-2/PGE2 signalling in hypoxia-induced angiogenic response in endothelial cells. J Cell Mol Med. 2012;16(8):1840–55. https://doi.org/10.1111/j.1582-4934.2011.01479.x. (**PMID: 22050691 PMCID: PMC3822696**).

32. Zhang X, Li Y, Ma Y, Yang L, Wang T, Meng X, Zong Z, Sun X, Hua X, Li H. Yes-associated protein (YAP) binds to HIF-1α and sustains HIF-1α protein stability to promote hepatocellular carcinoma cell glycolysis under hypoxic stress. J Exp Clin Cancer Res. 2018;37(1):216. https://doi.org/10.1186/s13046-018-0892-2. (**PMID: 30180863 PMCID: PMC6123950**).

33. Francisco Fernandez M, Charfi C, Piloto-Ferrer J, Lidia González M, Lamy S, Annabi B. Targeting ovarian cancer cell cytotoxic drug resistance phenotype with *Xanthium strumarium* L. Extract Evid Based Complement Alternat Med. 2019;15(2019):6073019. https://doi.org/10.1155/2019/6073019. (**PMID: 31827554 PMCID: PMC6885198**).

34. Berenguer A, Osoria L, González Suarez N, Manso A, Salomón S, Padrón Yaquis AS, Annabi B, Piloto-Ferrer J. Exploring the potential of Xanthatin from cuban *Xanthium strumarium*: isolation, characterization, and biological evaluation. J Biomed Res Environ Sci. 2024;5(9):1176–86. https://doi.org/10.37871/jbres2006.

35. Hanahan D. Hallmarks of cancer: new dimensions. Cancer Discov. 2022;12(1):31–46. https://doi.org/10.1158/2159-8290.CD-21-1059. (**PMID: 35022204**).

36. He R, Liu Y, Fu W, He X, Liu S, Xiao D, Tao Y. Mechanisms and cross-talk of regulated cell death and their epigenetic modifications in tumor progression. Mol Cancer. 2024;23(1):267. https://doi.org/10.1186/s12943-024-02172-y. (**PMID: 39614268 PMCID: PMC11606237**).

37. Sazonova EV, Chesnokov MS, Zhivotovsky B, Kopeina GS. Drug toxicity assessment: cell proliferation versus cell death. Cell Death Discov. 2022;8(1):417. https://doi.org/10.1038/s41420-022-01207-x. (**PMID: 36241623 PMCID: PMC9568594**).

38. Ling T, Lang WH, Maier J, Quintana Centurion M, Rivas F. Cytostatic and cytotoxic natural products against cancer cell models. Molecules. 2019;24(10):2012. https://doi.org/10.3390/molecules24102012. (**PMID: 31130671 PMCID: PMC6571673**).

39. Senrung A, Lalwani S, Janjua D, et al. 3D tumor spheroids: morphological alterations a yardstick to anti-cancer drug response. In vitro models. 2023;2:219–48. https://doi.org/10.1007/s44164-023-00059-8.

40. Zanoni M, Piccinini F, Arienti C, Zamagni A, Santi S, Polico R, Bevilacqua A, Tesei A. 3D tumor spheroid models for in vitro therapeutic screening: a systematic approach to enhance the biological relevance of data obtained. Sci Rep. 2016;11(6):19103. https://doi.org/10.1038/srep19103. (**PMID: 26752500 PMCID: PMC4707510**).

41. Edwardson DW, Parissenti AM, Kovala AT. Chemotherapy and inflammatory cytokine signalling in cancer cells and the tumour microenvironment. Adv Exp Med Biol. 2019;1152:173–215. https://doi.org/10.1007/978-3-030-20301-6_9. (**PMID: 31456184**).

42. Sio SW, Ang SF, Lu J, Moochhala S, Bhatia M. Substance P upregulates cyclooxygenase-2 and prostaglandin E metabolite by activating ERK1/2 and NF-kappaB in a mouse model of burn-induced remote acute lung injury. J Immunol. 2010;185(10):6265–76. https://doi.org/10.4049/jimmunol.1001739. (**Epub 2010 Oct 6 PMID: 20926798**).

43. Francou A, Anderson KV. The epithelial-to-mesenchymal transition (EMT) in development and cancer. Annu Rev Cancer Biol. 2020;4:197–220. https://doi.org/10.1146/annurev-cancerbio-030518-055425. (**Epub 2019 Nov 25 PMID: 34113749 PMCID: PMC8189433**).

44. Liaghat M, Ferdousmakan S, Mortazavi SH, Yahyazadeh S, Irani A, Banihashemi S, Seyedi Asl FS, Akbari A, Farzam F, Aziziyan F, Bakhtiyari M, Arghavani MJ, Zalpoor H, Nabi-Afjadi M. The impact of epithelial-mesenchymal transition (EMT) induced by metabolic processes and intracellular signaling pathways on chemo-resistance, metastasis, and recurrence in solid tumors. Cell Commun Signal. 2024;22(1):575. https://doi.org/10.1186/s12964-024-01957-4. (**PMID: 39623377 PMCID: PMC11610171**).

45. Georgakopoulos-Soares I, Chartoumpekis DV, Kyriazopoulou V, Zaravinos A. EMT factors and metabolic pathways in cancer. Front Oncol. 2020;7(10):499. https://doi.org/10.3389/fonc.2020.00499. (**PMID: 32318352 PMCID: PMC7154126**).

46. Zuo J, Wen J, Lei M, Wen M, Li S, Lv X, Luo Z, Wen G. Hypoxia promotes the invasion and metastasis of laryngeal cancer cells via EMT. Med Oncol. 2016;33(2):15. https://doi.org/10.1007/s12032-015-0716-65. (**Epub 2016 Jan 9 PMID: 26749588**).

47. Tsai YP, Wu KJ. Hypoxia-regulated target genes implicated in tumor metastasis. J Biomed Sci. 2012;19(1):102. https://doi.org/10.1186/1423-0127-19-102. (**PMID: 23241400 PMCID: PMC3541338**).

48. Xing Y, Wang R, Chen D, Mao J, Shi R, Wu Z, Kang J, Tian W, Zhang C. COX2 is involved in hypoxia-induced TNF-α expression in osteoblast. Sci Rep. 2015;12(5):10020. https://doi.org/10.1038/srep10020. (**PMID: 26066979 PMCID: PMC4464352**).

49. Hapke RY, Haake SM. Hypoxia-induced epithelial to mesenchymal transition in cancer. Cancer Lett. 2020;1(487):10–20. https://doi.org/10.1016/j.canlet.2020.05.012. (**Epub 2020 May 26 PMID: 32470488 PMCID: PMC7336507**).

50. Shi R, Liao C, Zhang Q. Hypoxia-driven effects in cancer: characterization, mechanisms, and therapeutic implications. Cells. 2021;10(3):678. https://doi.org/10.3390/cells10030678. (**PMID: 33808542 PMCID: PMC8003323**).

51. Calzada MJ, del Peso L. Hypoxia-inducible factors and cancer. Clin Transl Oncol. 2007;9(5):278–89. https://doi.org/10.1007/s12094-007-0055-y. (**PMID: 17525038**).

52. Kodaka M, Hata Y. The mammalian Hippo pathway: regulation and function of YAP1 and TAZ. Cell Mol Life Sci. 2015;72(2):285–306. https://doi.org/10.1007/s00018-014-1742-9. (**Epub 2014 Sep 30. PMID: 25266986 PMCID: PMC11113917**).

53. Wang X, Valls AF, Schermann G, Shen Y, Moya IM, Castro L, Urban S, Solecki GM, Winkler F, Riedemann L, Jain RK, Mazzone M, Schmidt T, Fischer T, Halder G, Ruiz Almodóvar de C. YAP/TAZ orchestrate VEGF signaling during developmental angiogenesis. Dev Cell. 2017;42(5):462-478.e7. https://doi.org/10.1016/j.devcel.2017.08.002. (**Epub 2017 Aug 31 PMID: 28867486**).

54. Li X, Cho YS, Zhu J, Zhuo S, Jiang J. The Hippo pathway effector YAP inhibits HIF2 signaling and ccRCC tumor growth. Cell Discov. 2022;8(1):103. https://doi.org/10.1038/s41421-022-00465-4. (**PMID: 36202785 PMCID: PMC9537283**).

55. Jun JC, Rathore A, Younas H, Gilkes D, Polotsky VY. Hypoxia-Inducible Factors and Cancer. Curr Sleep Med Rep. 2017;3(1):1–10. https://doi.org/10.1007/s40675-017-0062-7. (**Epub 2017 Jan 28 PMID: 28944164 PMCID: PMC5607450**).

56. Yi M, Li T, Niu M, Zhang H, Wu Y, Wu K, Dai Z. Targeting cytokine and chemokine signaling pathways for cancer therapy. Signal Transduct Target Ther. 2024;9(1):176. https://doi.org/10.1038/s41392-024-01868-3. (**PMID: 39034318 PMCID: PMC11275440**).

57. Zayed G, Mohammed H, Osman S. Nanocrustallization of dapsone; A novel approach to boost solubility, dissolution, and in-vitro anti-inflammatory activity. Al-Azhar J Pharm Sci. 2022;66(2):1–28. https://doi.org/10.21608/ajps.2022.268247.

58. Bai M, Yang M, Gong J, et al. Progress and principle of drug nanocrystals for tumor targeted delivery. AAPS PharmSciTech. 2022;23:41. https://doi.org/10.1208/s12249-021-02200-w.

59. Kohli K, Pillarisetty VG, Kim TS. Key chemokines direct migration of immune cells in solid tumors. Cancer Gene Ther. 2022;29(1):10–21. https://doi.org/10.1038/s41417-021-00303-x. (**Epub 2021 Feb 18 PMID: 33603130 PMCID: PMC8761573**).

60. Zajkowska M, Dulewicz M, Kulczyńska-Przybik A, Safiejko K, Juchimiuk M, Konopko M, Kozłowski L, Mroczko B. The significance of selected C-C motif chemokine ligands in colorectal cancer patients. J Clin Med. 2022;11(7):1794. https://doi.org/10.3390/jcm11071794. (**PMID: 35407400 PMCID: PMC8999061**).

61. Sarvaiya PJ, Guo D, Ulasov I, Gabikian P, Lesniak MS. Chemokines in tumor progression and metastasis. Oncotarget. 2013;4(12):2171–85. https://doi.org/10.18632/oncotarget.1426. (**PMID: 24259307 PMCID: PMC3926818**).

62. Bikfalvi A, Billottet C. The CC and CXC chemokines: major regulators of tumor progression and the tumor microenvironment. Am J Physiol Cell Physiol. 2020;318(3):C542–54. https://doi.org/10.1152/ajpcell.00378.2019. (**Epub 2020 Jan 8 PMID: 31913695 PMCID: PMC7099520**).

63. Rodríguez-Barbero A, Dorado F, Velasco S, Pandiella A, Banas B, López-Novoa JM. TGF-beta1 induces COX-2 expression and PGE2 synthesis through MAPK and PI3K pathways in human mesangial cells. Kidney Int. 2006;70(5):901–9. https://doi.org/10.1038/sj.ki.5001626. (**Epub 2006 Jul 5 PMID: 16820791**).

64. Shin S, Buel GR, Nagiec MJ, Han MJ, Roux PP, Blenis J, Yoon SO. ERK2 regulates epithelial-to-mesenchymal plasticity through DOCK10-dependent Rac1/FoxO1 activation. Proc Natl Acad Sci U S A. 2019;116(8):2967–76. https://doi.org/10.1073/pnas.1811923116. (**Epub 2019 Feb 6 PMID: 30728292 PMCID: PMC6386703**).

65. Tabei Y, Nakajima Y. IL-1β-activated PI3K/AKT and MEK/ERK pathways coordinately promote induction of partial epithelial-mesenchymal transition. Cell Commun Signal. 2024;22(1):392. https://doi.org/10.1186/s12964-024-01775-8. (**PMID: 39118068 PMCID: PMC11308217**).

66. Greenhough A, Smartt HJ, Moore AE, Roberts HR, Williams AC, Paraskeva C, Kaidi A. The COX-2/PGE2 pathway: key roles in the hallmarks of cancer and adaptation to the tumour microenvironment. Carcinogenesis. 2009;30(3):377–86. https://doi.org/10.1093/carcin/bgp014. (**Epub 2009 Jan 9 PMID: 19136477**).

67. Limame R, Wouters A, Pauwels B, Fransen E, Peeters M, Lardon F, De Wever O, Pauwels P. Comparative analysis of dynamic cell viability, migration and invasion assessments by novel real-time technology and classic endpoint assays. PLoS ONE. 2012;7(10):e46536. https://doi.org/10.1371/journal.pone.0046536. (**Epub 2012 Oct 19 PMID: 23094027 PMCID: PMC3477108**).

Discover